Ralph J. Roberts
CENTER FOR RESEARCH
IN
ECONOMIC GEOLOGY

ANNUAL RESEARCH MEETING-1998

Program and Reports

7-8 January 1999
Midby-Byron Building
Room 107-109
University of Nevada, Reno
Reno, NV 89557

The Rain Mine Gold-bearing Breccia System
Part I: Field Relationships

Cindy L. Williams[1]
Tommy B. Thompson[2]
Jon L. Powell[1]
W. Warren Dunbar[1]

[1]Newmont Gold Co., Rain Mine, P.O. Box 669, Carlin, NV 89822
[2]Center for Research in Economic Geology (CREG), Mackay School of Mines/169
University of Nevada, Reno; Reno, NV 89557-0232
e-Mail: tommyt@mines.unr.edu

THE RAIN MINE GOLD-BEARING BRECCIA SYSTEM
PART I: FIELD RELATIONSHIPS

Cindy L. Williams[1]
Tommy B. Thompson[2]
Jon L. Powell[1]
W. Warren Dunbar[1]
[1]Newmont Gold Co., Rain Mine, P.O. Box 669, Carlin, NV 89822
[2]Center for Research in Economic Geology (CREG), Mackay School of Mines/169
University of Nevada, Reno; Reno, NV 89557-0232

Abstract

The Rain mineral system includes a mined-out 1.17 million ounce open pit reserve at 1.8 g/t gold and rapidly increasing underground reserves plus past production estimated at 157,000 ounces gold averaging 7.7 g/t. Rain orebodies are hosted at the Devils Gate Limestone-Webb Formation contact in a breccia complex within the hanging wall of the Rain fault.

Structure in the system is dominated by two fault sets: the northwest-striking Rain fault system and a northeast-striking fault set. The Rain fault is interpreted as a right-lateral, dominantly strike-slip fault with classic extensional and compressional flower structures developed in its hanging wall. The northeast-striking faults are interpreted as conjugate left-lateral strike-slip faults with post-mineral normal reactivation and formation of additional synthetic and antithetic faults during Basin and Range extension. Both fault sets control mineralization, although the Rain and sub-parallel faults served as the primary feeders. Unusually wide ore zones coincide with flower structures. Rain mine exposures provide the most convincing evidence to date for a right-lateral strike-slip fault system as a critical component in formation of a Carlin Trend orebody.

The Rain orebody is hosted entirely within a wedge-shaped breccia body above the Devils Gate Limestone-Webb Formation contact. The system includes four texturally and genetically distinct breccia types: hydrothermal crackle, fluidized hydrothermal, hydrothermal accretionary lapilli and tuffisite, and collapse breccias. Pre- and syn-ore hydrothermal breccias formed due to at least three

episodes of boiling, overpressuring and convective fluidization, followed by mineral cementation (sealing) by the remnant supersaturated hydrothermal fluid. High-grade gold was deposited as a late phase ponded at the top of the hydrothermal and crackle breccias.

The Rain orebody results from 5 interpreted stages of development: (1) structural preparation along the right-lateral Rain strike-slip fault system and conjugate left-lateral northeast-striking faults; (2) multiple episodes of fluidized hydrothermal breccia, with high grade gold deposition immediately following the last breccia event; (3) late channelized fluidized rock fragments and fine clays forming accretionary lapilli and tuffisite bodies; (4) post-mineral normal reactivation of structures; and (5) collapse brecciation resulting from post-ore acidic fluid ponding on and dissolution of the upper Devils Gate Limestone.

On a worldwide scale the Rain system is unique with hydrothermal breccias extending >5 km along strike. This Part One paper lays the foundation for future work on Rain refractory ores, gold residence, thermal and geochemical zoning, the relationship between oxide and refractory ores, and the role of organic carbon.

Introduction

The southern Carlin Trend's Rain mine is 29 kilometers south of Carlin in Elko County, Nevada (Fig. 1). The Rain hydrothermal system includes, from southeast to northwest, small oxide gold inventories at Snow Peak and BJ Hill, the mined-out Rain pit, the Rain underground mine, and underground inventories including Northwest Rain and Tess.

Although it is considered the southern end of the Carlin Trend, the Rain system is unique compared to other "Carlin-type" gold deposits. The system is hosted by a fluidized hydrothermal breccia that extends at least five kilometers along the Rain fault. A fluidized breccia of such lateral extent is not only unique on the Carlin Trend, but also unusual in other worldwide systems.

This paper is the first of a two-part study. Part I documents field relationships including stratigraphy, structure, breccia body geometries, textures and interpreted origins, gold orebody geometry, oxide mineralogy and paragenesis, relation to breccias, and the relative timing of all events. The current data have been collated into a 5-stage model of breccia and ore formation. Part I data are from: (1) current observations and interpretation by Newmont Gold Co. mine and exploration geologists; (2) 1997 field and lab work by one of us (TBT); (3) observations from previously involved Newmont geologists; and (4) an M.S. thesis (Williams, 1992).

Part II, scheduled for 1999 completion, will stem from M.S. research at the University of Nevada, Reno, as part of industry-supported CREG research. The studies will build on Part I by adding petrographic, fluid inclusion, Scanning Electron Miscoscope (SEM), microprobe and stable isotope analyses. The new data should: (1) characterize refractory ore mineralogy and paragenesis and evaluate changes between oxide and refractory ores, including the question of gold residence; (2) characterize the nature and source of ore fluids (*i.e.* resolve the supergene versus hypogene question about the origin of deep oxide ore); (3) determine if any thermal gradients are present in the hydrothermal system; (4) evaluate trace element dispersion along the faults (plumbing); (5) document the role of organic carbon in the system; and (6) generate a computer model for the formation of the Rain hydrothermal system.

History and Gold Endowment

Newmont discovered Rain in 1979 after a property submittal by P. Montrose (Knutsen and West, 1984). The discovery outcrop was a jasperoid ridge along the Rain fault. The jasperoid contained massive barite, alunite and gold values up to 17 parts per billion (ppb). Delineation drilling began in 1981. By 1987 an open pit-minable reserve of 22.5 million tons at 1.8 gram/tonne (g/t) gold, or 1.17 M ounces, was defined. The open pit reserve was mined-out between 1987 and 1994.

Gold mineralization extending along the Rain fault northwest of the ultimate Rain pit highwall was first evaluated by R. Thoreson in 1990. The ore pod was too small to support the high strip ratio required, and was therefore evaluated as a potential underground operation. In October 1993, two portals collared in the northwest Rain pit highwall began the Carlin Trend's first underground mine. The operation was intended to extract a 7,000 ounce underground oxide reserve before cessation of open pit mining and subsequent mill shut down.

Newmont's exploration team, originally led by D. Mathewson and later by M. Jones, T. Longo and J. Read, has successfully continued defining the system to the northwest. Underground core drilling and development, previously led by M. Lane and D. Heitt, has gradually converted these extensions to underground reserves. By January 1996, reported oxide reserves plus production totaled 157,150 ounces at 7.7 g/t. The reserve is currently divided into four areas: Stopes 1 and 2 and Zones 3 and 4. Excellent potential exists to continue expanding underground reserves to the northwest.

Regional Geology

The Rain mine is on the Carlin Trend, a 60-kilometer-long alignment of sedimentary-rock-hosted gold deposits trending north-northwest across northeastern Nevada (Fig. 1). Past gold production, reserves and resources on the Carlin Trend currently total 107 million troy ounces (Teal and Jackson, 1997). Carlin Trend regional geology is documented by Teal and Jackson (1997) and Christensen (1993) and will only be summarized here.

During the Paleozoic era, northeastern Nevada was located along the stable western North American continental margin. Western eugeoclinal and eastern miogeoclinal sediments were deposited as interfingering packages on the continental shelf and slope. During the Late Devonian to Early Mississippian Antler orogeny, western-facies siliceous rocks were placed over eastern-facies

carbonates along the Roberts Mountains thrust fault (Smith and Ketner, 1968). Fine- to coarse-grained siliceous sedimentary rocks eroded from the emerging highland, formed the Middle Mississippian to Early Pennsylvanian overlap assemblage (Smith and Ketner, 1975).

Subsequent compressional tectonic events from Late Paleozoic (Humbolt Orogeny) through Mesozoic (Sonoma and Sevier Orogenies) time resulted in further complex uplift, folding and thrusting (Stewart, 1980). Igneous events are documented as late Jurassic (158 Ma Goldstrike stock) and late to early Oligocene (35-40 Ma dikes and sills) by Arehart (1993), Smith and Ketner (1975), and Emsbo *et al.* (1996). Extensional tectonism began as early as 40 Ma, with true Basin and Range extension starting at 20 Ma (Evans, 1980). Early compressional events followed by Basin and Range extension and erosion created windows of eastern facies carbonate rock through the siliceous upper plate rocks. All currently known Carlin Trend gold deposits occur within or proximal to these lower plate carbonate windows (Teal and Jackson, 1997).

Although the Rain mine is located in a lower plate window block, it differs from other Carlin Trend deposits because it is hosted in Mississippian overlap assemblage rocks, rather than lower plate Siluro-Devonian carbonate rocks.

Rain District Rock Units

The oldest unit exposed in the Rain mine is the autochthonous lower plate 150 to 200 m thick Devonian Devils Gate Limestone. The unit is a medium- to thick-bedded micritic limestone with local stromatoporoid colonies, horn corals and fossil hash (Fig. 2).

The overlap-assemblage Mississippian Webb Formation unconformably overlies the Devonian Devils Gate Limestone. The limestone surface was exposed to erosion, and karst features developed regionally prior to Webb Formation deposition. A terra rossa clay is common at the contact.

Anomalous gold values and relatively small (<1 M ounce) gold deposits are also common at the Devils Gate-Webb (or equivalent units) boundary throughout the eastern Great Basin (Maher, 1997).

Webb Formation sedimentary rocks include thinly-bedded mudstone and siltstone with local channel sand and conglomerate lenses. The unit is 120 to 150 m thick. Webb Formation units are carbonaceous and locally exhibit turbidite cross-bedding and soft sediment deformation.

The Webb Formation coarsens upward through a gradational contact with the Mississippian Chainman Formation. Chainman sedimentary units consist of medium- to coarse-grained sandstone and local conglomerate. The unit is 400 to 500 m thick and also coarsens upward. Webb and Chainman Formation rocks span depositional environments from pre-orogenic deep-water sedimentation to early-orogenic overlap assemblages.

The allochthonous Devonian Woodruff Formation overlies the eastern- and overlap-assemblage sedimentary rocks. The unit includes thin-bedded siltstone and mudstone with diagnostic phosphate nodules. The rocks are pervasively folded and internally deformed. Woodruff Formation units range from 90 to 350 m thick.

Structure

Introduction

Two fault sets dominate Rain structural geology: the northwest-striking Rain fault system and a northeast-striking set. The Rain fault system strikes N40-50°W in the open pit but shifts more westerly in the underground exposures (N65-85°W), and the northeast set strikes N0-40°E (Figs. 3 to 5). The Rain fault dips 68-80°SW in the open pit but to the northwest in the underground exposures it flattens to 45°W; the northeast-striking faults dip northwesterly (45-78°). The Rain fault system is the primary control on gold mineralization, but some northeast faults were also secondary conduits for mineralizing fluids.

Although the two high-angle fault sets are most important to mineralization, the Rain subdistrict also includes Roberts Mountains thrust-associated low-angle faults and folds. Although evidence for this is most prevalent in the pervasively-sheared and folded allochthonous Woodruff Formation, low-angle faults are also present in the Webb Formation sedimentary rocks overlying ore. They may be affiliated with Antler Orogeny compressional tectonics or with Rain fault-associated drag folding and bedding plane slip. Although they pre-date mineralization, these low-angle faults did not significantly affect mineralization.

Rain Fault System

The Rain fault system is the district's dominant structure in terms of offset and importance as a mineralizing fluid conduit. At district-scale the fault strikes N40-50°W and is traceable for more than eleven kilometers. Dips are consistently to the southwest, but dip amounts range from 68-80°SW in the Rain pit to 38-45°SW less than 450 m northwest of the pit. The fault places barren Woodruff Formation rocks against the Devils Gate Limestone-Webb Formation contact with at least 625 m of apparent reverse displacement (Figs. 3 and 6). Mineralization is localized in the Rain fault hanging wall, immediately above the Webb Formation-Devils Gate Limestone contact. At ore levels, the Rain fault occurs as less than 3 cm of crushed rock separating barren Woodruff rocks from ore-bearing breccias. The fault is healed by the mineralizing event with only minor evidence of post-mineral offset.

En echelon Rain sub-parallel faults were recognized in the Rain pit, but recent underground exposures have documented more and provided information on their significance (Figs. 3-6). These faults include the Galen in the Rain pit and the Revelation, Flower, Phantom and Hidden in underground Zones 3 and 4. The structures diverge 10-20° from the Rain fault, striking N75-85°W. Instead of splaying off of the Rain fault, however, the faults occur as non-connected en echelon

segments less than 470 m long. The Flower, Galen and Hidden faults dip southwest 55-85°, sub-parallel to the Rain fault. Conversely, the Phantom and Revelation dip 50-60° northeast toward the Rain fault. In Zones 3 and 4 the resultant geometry is a series of blocks uplifted and flaring outward on convex-up structures, a classic positive flower structure as defined by Wilcox *et al.* (1973) (Fig. 7). The positive flower explains the seemingly extreme variation in Rain fault dips from 85° to 38°. The shallower structure in Zone 4 is a flatter fault branching off the primary Rain fault at depth, forming the right or northeast side of a symmetrical flower structure (Fig. 7). Recent underground exposures suggest the Rain fault strike may change from N65°W in Zone 3 to N85°W between Zones 3 and 4, forming a left-hand bend.

A weakly-developed negative flower structure is also interpreted in the Rain pit (Figs. 3, 4, and 6). The Galen fault and a second Rain sub-parallel structure, inferred from breccia, alteration and orebody geometries, form what appears to be a down-dropped block in the Rain fault hanging-wall. The geometry of the possible negative flower structure, however, is partially obscured by hydrothermal breccias. Historic Rain pit level-plan maps indicated that, adjacent to the interpreted negative flower structure, the Rain fault bends northward from N65°W to N35°W.

Rain sub-parallel fault exposures in Zone 3 and 4 orebodies are subtle. The aptly named Phantom fault is expressed as a set of fractures less than 2 cm-wide, forming a 2 meter-wide zone. Displacement on the Devils Gate Limestone-Webb Formation contact is less than 6 m and post-ore offset is indeterminant due to contrasting ore thickness across the fault (Fig. 7). Despite unimpressive exposures, the Phantom fault juxtaposes 17.1 g/t breccia with visually identical but virtually barren breccia. The Revelation occurs as a 15 to 35 m-wide weakly argillized zone of minor southwest- and northeast-dipping shears and anastomosing tuffisite dikes and sills from several centimeters to 5 m-wide. The structure dips toward the Rain fault and has 15 m of apparent reverse

offset on the Devils Gate Limestone surface. Again, orebody offset is uncertain because ore is thin or absent in the hanging wall and more than 30 m thick in the footwall (Fig. 7). The Flower fault dips southwest with the Rain fault and exhibits apparent reverse displacement of 18 m on the Devils Gate Limestone-Webb Formation contact, but 6 m of normal offset on mineralization. The orebody is locally thicker on the footwall but higher grade in the hanging wall. Finally, the Hidden fault dips sub-parallel to the Rain fault. The structure is consistently tuffisite-filled, but shows little apparent displacement of ore.

Attempts at palinspastic restoration of Rain fault set structures in two-dimensional cross sections reveal problems with volume loss and gain. These problems cannot be rectified without moving material in and out of the section plane. Such space problems are commonly associated with strike-slip displacement (Sylvester, 1988).

Folds provide additional information on the Rain fault history. In the Rain pit the asymmetrical Kilo anticline occurs in the Rain fault hanging wall (Fig. 4). The fold axis diverges from the Rain fault in the southern-most exposures. Other folds in the hanging wall rocks are broad open folds trending southwest with shallow plunges. In contrast, the footwall rocks are strongly folded into south-plunging asymmetrical folds at considerable distances from the Rain fault and oriented perpendicular to the Antler-related principal stress field; the consistent southward plunge suggests that the footwall block has been rotated after the folds formed. In close proximity to the Rain or sub-parallel faults, the folds have been rotated to southwest- or west-southwest orientations, consistent with drag associated with right-lateral separation.

The Rain fault system was present during mineralization, forming conduits for gold-bearing hydrothermal fluids. The hydrothermal system follows the Rain fault. Rain sub-parallel faults strongly influence gold grade distribution, although the faults themselves are commonly low grade

Near the Rain and Rain sub-parallel faults, northeast fault geometries become even more complex. Anastomosing northeast-striking faults may be spaced every 3 m, and dramatic strike and dip changes occur over short distances. The northeast-striking structures always offset the Rain fault. However, locally the northeast set may be offset by Rain sub-parallel faults, or offsets between the two may be mutual. In one case, reverse offset of a northeast-striking fault by the Rain sub-parallel Flower fault is documented.

The northeast fault set can be divided into two groups: one clearly influencing and offsetting mineralization and the other clearly post-mineral and only offsetting the orebody. Approximately 20% of northeast-striking faults controlled and enhanced hydrothermal brecciation and mineralization (Figs. 10 and 11). A strong ore grade and thickness enrichment occurs in the Pyrite fault footwall. In the Rain pit, zones of fluidized hydrothermal breccia clearly stoped up along the Sharpstone fault which also shows sharply enhanced ore grade and thickness in its hanging wall. Some northeast-striking faults also form breaks where ore shifts laterally across the fault. For example, across the Shop fault ore shifts from a Rain parallel fault on the southeast to lie against the Rain fault on the northwest (Figs. 10 and 11). The remaining 80% of northeast structures had no influence on mineralization, forming later during an extensional event.

Stereonet Solutions to Rain Fault System

Differences in bedding attitudes on either side of the Rain fault are distinct (Fig. 9); the hanging wall rocks of the Webb Formation exhibit very consistent northwest strikes with low to moderate southwest dips and southwest-plunging open folds (Fig. 9-A). In contrast, the footwall Woodruff Formation rocks are strongly folded (Fig. 9-B), reflecting a complicated structural history. In general, these rocks exhibit steep southwest to flat dips (Fig. 4) but are strongly folded into south-plunging and west-plunging asymmetrical folds.

Stereonet analyses indicate the average Flower fault attitude lies at a true angular separation of 14° from the average Rain fault orientation. The geometry suggests that it may have formed as a synthetic or Riedel shear during Rain fault strike-slip motion. If so, a stereonet solution indicates a 13° S51°E slip-line direction or right-lateral reverse oblique displacement on the Rain fault (Fig. 9-D). Similarly, the Rain and Revelation faults' slip-line solution is 3° S58°E. Similar stereonet analyses for the Rain open pit area yield rake solutions on the Rain fault of 25-35° S51-56°E or right-lateral reverse oblique separation (Fig. 9-C). Observed slickenlines on the Rain fault in the open pit rake 17-30°S. Stereonet solution of the average Rain fault attitude and average orientations of 50 northeast-striking fault planes (type-examples of ore-controlling northeast structures) yields a true angular separation of 63°, suggesting conjugate geometry (Fig. 9-B). Notably similar to the Rain and Rain sub-parallel fault solutions, the slip-line direction is 10° S48°E, again indicating dominantly strike-slip movement. Within the open pit area the northeast-striking and Rain faults yield theoretical slip-line directions of 12-15° N27-48°E, suggesting left-lateral separation (Fig. 9-C). Most observed rakes range between 16-66°NE.

A local stress field developed in the zone of transpression (Figs. 9-D, -E) that reflects the local change in strike and dip along the Rain and northeast-striking faults; the principal shortening axis is oriented N28°W at -13°.

Structural Genesis

Mutually offsetting and complex intersections between the Rain fault system and ore-controlling northeast-striking faults and true angular separations of 60 to 75° suggest the two formed as a conjugate set. Fault geometries, flower structures, fold orientations and kinematic indicators provide strong evidence for formation in a pure shear right-lateral transpressional environment as defined by Sylvester (1988).

Rain subdistrict fault geometries are similar to simple-shear models for strike-slip fault systems (Sylvester, 1988) (Fig. 9-A, -B and -C). The primary structure is the N65-75°W Rain fault. The Rain sub-parallel fault set strikes 10-20° west (14° true angular separation from stereonet solution) from the primary Rain fault; an orientation consistent with pinnate or synthetic strike-slip shears (Tchalenko and Ambraseys, 1970; Sylvester, 1988). At 13° S51°E, the stereonet slip-line solution for the Rain and Rain sub-parallel faults supports dominantly right-lateral strike-slip movement. The ore-controlling northeast-striking faults are oriented at 63° true angular separation from the Rain fault. The orientation matches the 60-75° angle Sylvester (1988) predicts for conjugate or antithetic shears, with shear sense opposite the primary structure. Although conjugate shears are not commonly observed (Sylvester,1988), the similar slip line for the Rain fault and the ore-controlling northeast-striking Pyrite and Barite faults (10° S48°E) compared to the Rain and Rain sub-parallel set (13° S51°E) indicates they formed during the same strike-slip displacement. Thrust fault orientations in the Rain footwall rocks indicate south-directed compression based on south-vergent fold axes adjacent to the thrusts. The modification of Antler-related fold orientations by later tilting and shear-related rotation of axes is consistent with shear-related modification of the older folds.

A second strong argument for a strike-slip component to Rain fault formation is the presence of flower structures. Transpression or converging strike-slip (on a fault bend)(Fig. 9-E) provides a component of horizontal shortening, yielding compensatory uplift of fault zone rocks. The result is a series of slabs that rise upward and outward on convex-up faults over the adjacent blocks like stacked imbricate thrusts (Sylvester, 1988). This arrangement was first termed a positive flower structure by Wilcox *et al.* (1973). The Zone 4 positive flower structure is well-documented by underground exposures and drill data. Recent exposures suggest a left-hand Rain fault bend where the Zone 4 flower appears, a geometry consistent with right-lateral Rain fault offset. The inferred

Rain pit negative flower structure occurs at a right-hand fault bend, similarly supporting right-lateral transtensional motion.

In addition, assuming the ore-controlling northeast-striking faults and the Rain fault formed as a conjugate set, stereonet analysis indicates a principal stress direction (sigma one) 0-10°S7°W, an orientation that would yield right-lateral strike-slip movement on the Rain fault set and left-lateral strike-slip motion on the antithetic conjugate northeast-striking set (Figs. 9-C, -D, and -E). Finally, slickenlines on both fault sets locally show low-angle slip directions, consistent with the projected stereonet solutions. The ore-controlling northeast-striking faults are interpreted as antithetic faults conjugate to the dominant right-lateral Rain fault. However, early motion on both northeast- and northwest-striking fault sets is clearly overprinted by post-ore listric normal displacement, which is especially strong on the northeast faults. While an estimated 20% of the northeast-striking faults formed as Rain fault conjugates, the remainder formed as synthetic and antithetic structures accommodating later extensional offset and block rotation. The post-ore movement is associated with Basin and Range extension, regionally estimated at 64-100% (Wernicke and Birchfiel, 1982). The final northeast-striking fault set geometries agree well with Basin and Range listric normal fault models proposed by Gans *et al.* (1985), Profett (1977), and Wernicke and Birchfiel (1982).

Regional Implications of an Ore-Controlling Right-Lateral Event

Transpressional right-lateral motion on the Rain fault systems would have required northwest-southeast compression which could be expected to regionally form similar faults. In fact, nearly identical deformation with ore-controlling northwest-striking faults and folds has been documented south of Rain in the Alligator Ridge area (Nutt, 1997). Nutt (1997), however, interprets the movement as sinistral rather than dextral. The work, though, is based on limited data from regional mapping. The Gold Quarry mine (23 km north of the Rain mine) is strongly influenced by a dominant

pipe and the pipe walls. Such slumping is common in lapilli pipes due to periodic decreased fluid pressure and subsequent compaction (McCallum, 1985).

The consolidated breccia was cut by vertically-elongate bodies of poorly consolidated lapilli exhibiting only minor compactional deformation. Contacts with the consolidated lapilli breccia were sharp and scoured. All material within the accretionary lapilli pipe was cut by extensional en echelon gash fractures, again resulting from compaction during pressure decrease.

Accretionary lapilli zones several centimeters to several meters wide are also observed in underground drill core. The tuffisite dikes exhibit local accumulations of accretionary lapilli indicative of the fluidized origin of the dikes; most of the lapilli are intensely argillized and commonly are represented by spherical voids interspersed with white spherical clay masses less than 1mm in diameter. In all cases, accretionary lapilli zones cut the fluidized hydrothermal breccia body, locally extending beyond breccia contacts into Webb Formation sedimentary rocks. Lapilli zones have not been observed in the collapse breccia or the Devils Gate Limestone. Gold grades in lapilli zones are generally similar to or lower than grades in adjacent breccia units. In the Webb Formation, accretionary lapilli zones are higher grade than the adjacent barren (less than 0.2 g/t) sedimentary rocks. The field relationships indicate the lapilli zones formed after the last fluidized brecciation event, in channelized fluid conduits cutting up through the breccia mass along openings created by northwest- and northeast-striking faults and flat-lying extensional zones created by compaction in the fluidized breccias. Formation must have occurred as a late stage of breccia C, before the breccia mass was cemented with silica. It is not clear if they formed before or after the high-grade gold event.

Finally, rocks previously classified as intrusive are present in the Rain mine. In underground exposures these rocks cut ore-bearing breccia bodies, forming dike- and sill-like geometries focused on northwest- and northeast-striking fault sets. Exposures range from several centimeters to more

than 3 meters wide. The rocks are generally lower-grade than adjacent units, but locally assay as high as 8.6 g/t gold. The units are intensely argillized, masking primary textures. Recent petrographic work, however, documents that these "intrusives" are actually fragmental or injected rock flour units associated with the hydrothermal breccia system, and they are classified as "tuffisites". Locally, the tuffisites exhibit marginal banding that consists of alternating light- and dark-colored layers comprised of fine rock flour (light-colored) and sulfidic fragments (dark-colored); the interior portions of the tuffisite dikes are massive with no apparent fragment flow orientation. Sulfide fragments are common within the medial portions of the tuffisite dikes.

Collapse Breccia

The youngest breccia type present at Rain is collapse breccia. Collapse breccia forms an irregular blanket of variable thickness between the hydrothermal breccia and the Devils Gate Limestone (Fig. 12).

Collapse breccia geometry is irregular with thickness pinching and swelling from 52 to 60 m. The thickest zones are structurally localized, with collapse breccia stoping up into hydrothermal breccias and extending down into the Devils Gate Limestone contact. The upper collapse breccia contact is gradational from true collapse breccia into strongly fractured and argillized hydrothermal breccia. The lower contact is a gradation from unconsolidated collapse breccia into fractured and dolomitized limestone.

Collapse breccias are unconsolidated with local voids as much as 18 m high. Fragments are dominantly composed of overlying hydrothermal breccia with dolomitized limestone fragments occurring where breccias cut into the Devils Gate surface. Collapse breccias are fragment supported with I:F of 10:90 to 40:60. Matrix is invariably a red clay containing quartz, illite, and kaolinite with local jarosite, Fe- As- and Mn-oxides, alunite, siderite, dolomite, calcite and montmorillonite. The

red clay is interpreted as insoluble residues resulting from carbonate removal in the Devils Gate Limestone (Williams, 1992).

Collapse breccia is characterized by low gold grades, generally less than 1.7 g/t. In detail, fragments (breccias a, b and c) may be high grade (greater than 5.1 g/t), but the 10 to 40% clay matrix generally contains less than 0.3 g/t gold.

Gold Mineralization and Geochemistry

The entire Rain breccia body contains gold grades exceeding 0.3 g/t. The high-grade (>5.1 g/t) ore mined in the underground operation, however, is focused at the top of the breccia (Fig. 12). Sharp grade breaks between crackle breccia and overlying argillized Webb sedimentary units suggest ore-bearing fluids ponded beneath the impermeable clay zone. The high-grade gold event occurred after the last phase of fluidized brecciation, otherwise gold grade would be relatively homogeneous throughout the breccia. In addition to being ponded under an impermeable cap, gold mineralization was also influenced by the Rain sub-parallel faults and certain northeast-striking faults. The relationship between structures and grade is illustrated using grade times thickness (Fig. 10) and average grade (Fig. 11) contour maps.

In the Rain pit, elevated grade times thickness (GT) zones are controlled by the Rain-sub-parallel Galen fault, and breccia near the Rain fault is low grade. Grade times thickness and average grade are enhanced in the Sharpstone fault hanging wall, suggesting it also acted as a feeder. Where the orebody crosses the northeast-striking Shop fault near the portals, ore shifts from the Galen fault to the Rain fault. This geometry continues through Stopes 1 and 2 where the Rain fault appears to be the primary feeder.

In Zone 3 GT and grade contours again pull away from the Rain fault, favoring the Rain sub-parallel Revelation and Phantom faults. A thick and high grade pod at the northwest end of Zone 3

occurs in the Revelation fault footwall and against the northeast-striking Pyrite fault footwall (Figs. 10 and 11). In this case, both structural sets have augmented gold grades adjacent to them. In Zone 4, grade contours are strongly influenced by Rain sub-parallel faults, with higher grade in the Revelation fault footwall and the Flower and Hidden fault's hanging walls. Grade times thickness contours show the same trend, and also define a zone of distinctly lower GT in the argillized Revelation fault zone (even though the fault's footwall shows strongly enhanced GT). Grade is zoned with low grade contours in the Rain pit and much higher grades in Zone 4.

High gold values in Rain crackle and fluidized breccias are associated with enriched As, Hg, Sb and to a lesser extent Mo, Zn, Pb and V relative to unaltered Webb and Devils Gate sedimentary units (Williams, 1992). Relative to the earlier hydrothermal breccia, collapse breccia samples are strongly enriched in As, Hg, Co, Cu, Fe, Mn, Ni, V, Zn and Sb (Williams, 1992). Similar element enrichments are found in red clay fracture coatings throughout the hydrothermal breccia. All of these elements would be soluble in an acidic, oxidized fluid and readily precipitated with a pH increase (buffering). More detailed geochemical analysis will be included in Part II.

Nature of Rain Oxidation

The Rain hydrothermal breccia system can be divided into oxide and refractory zones. Currently, the nature of oxidation (hypogene or supergene) is unclear.

In the Rain pit and early underground workings, the breccia body is pervasively oxidized with only minor relict refractory pods. Acidic oxidizing fluids produced argillic alteration including replacement and vein alunite, kaolinite, jarosite, hematite, goethite, duessertite, scorodite, mansfieldite, willemite, montmorillonite (on the limestone contact), cinnabar, and halloysite. The timing and relative abundance of these minerals is shown in Figure 14.

Williams (1992) reported on sixteen samples of Rain pit sulfides and sulfates for sulfur isotope ratio analysis to determine hypogene versus supergene sulfate origin. The samples included diagenetic and hydrothermal pyrite, barite, alunite and jarosite. Field (1966) and Ohmoto and Rye (1979) note that sulfates produced from sulfides by supergene processes have essentially identical $\delta^{34}S$ values as the sulfides. In contrast, hypogene fluids yield sulfates with significantly higher $\delta^{34}S$ values than the diagenetic sulfides. In the Rain pit samples, barite $\delta^{34}S$ was enriched relative to sulfides (Fig. 15), indicating a hypogene origin. However, $\delta^{34}S$ values in alunite and jarosite were almost identical to sulfide values, indicating a supergene origin (Fig. 15). Supergene oxidation is also supported by very young, 12 to 22 Ma, potassium-argon dates from Rain pit alunite samples (Odekirk, 1989). With increasing depth, underground workings and core drill holes are encountering carbon-sulfide refractory ore. Mixed with refractory material is oxidized ore occurring below as much as 1,500 feet of unoxidized carbonaceous and sulfidic Webb and Chainman Formation sedimentary rocks. Oxide-refractory contacts range from sharp to gradational. Geostatistics for Zone 4 gold assays indicate refractory and oxide mineralization are part of the same population. Recent drill results further to the northwest, however, suggest that the refractory material may consistently be higher grade, possibly suggesting a separate mineral event or deposit-scale zoning.

Few would dispute that Rain pit ores experienced supergene oxidation, but the question remains if all Rain oxidation is supergene. Thick, unoxidized rock overlying oxide ores combined with locally sharp oxide-refractory contacts (suggesting a crosscutting event) raise questions about the origin of deep oxide ores. Little work has been done on refractory ore mineralogy, paragenesis and textures and their comparison to oxide ores. Completion of Part II research will add these critical data and help resolve the supergene versus hypogene debate.

Hydrothermal Alteration

The Rain system exhibits zoning of hydrothermal alteration minerals in hanging wall rocks as well as within the hydrothermal breccia mass. Prior to development of the hydrothermal breccia, the Webb Formation siltstones were silicified along bedding planes and faults adjacent to the Rain fault zone; locally, biotite and quartz replacement of siltstone occurred along bedding planes or in veinlets (Fig. 14). Unaltered Webb sedimentary rocks peripheral to the ore-bearing breccia grade into intensely argillized rock within 15 to 30 m of the orebody. The argillic zone is composed of mixed carbonaceous clays identified by x-ray diffraction as 4-43% illite, 0-17% kaolinite, and 0-13% montmorillonite (Williams, 1992). The argillic zone is interpreted to have formed during hydrothermal brecciation, before the main gold precipitation event. Argillically altered rock is in sharp contact with silicified and baritic breccia. The fluidized hydrothermal and crackle breccia zones are moderately to intensely silicified and replaced by barite. Silica content ranges from 40 to 95% and barite from 0 to 90%. Average barite content is zoned from southeast to northwest. Rain pit and Stope 1 and 2 ore is characterized by 30-40% average barite content. The average decreases to 20-30% in Zone 3, 10-20% in Zone 4 and 0-10% to the northwest beyond Zone 4. In lower portions of the breccia, silicified and baritic rocks grade downward into argillic assemblages, characterized as supergene products within the Rain pit, and dominated by kaolinite (17-38%), alunite (3-80%), illite (0-29%), jarosite (1-4%), residual quartz (26-81%) and barite (1-7%). Similar clay assemblages are present in the underground exposures, but their origin is not known. The argillic alteration overprints earlier silica and barite, forming as fracture fillings and alteration fronts extending into silicified and baritic breccias (Fig. 14). Argillized hydrothermal breccia grades downward into clay-matrix collapse breccias on the Devils Gate Limestone surface. Residual quartz (46-80%) and barite (2-7%) with minor kaolinite, alunite, montmorillonite (on the limestone contact), illite, calcite, siderite, jarosite and

iron oxide (3-6%) dominate collapse breccia matrix material. Both argillized breccia and the collapse breccia matrix also locally contain minor goethite, duessertite, scorodite, mansfieldite, willemite, cinnabar, and halloysite (Williams, 1992). Finally, Devils Gate Limestone under the breccia body is pervasively recrystallized and dolomitized. Carbonate species present include ferroan calcite and ferroan dolomite, in addition to dolomite.

A Rain System Formational Model

A five-stage formational model for development of the Rain mine breccias and gold orebody is detailed below. Fluid origins and the development of ore and rock oxidation are to be described in Part II of our studies on the geochemistry of the Rain ore system.

Stage One: Structural Preparation

The first stage in Rain development was right-lateral oblique movement on the Rain fault. Rain fault motion resulted in formation of synthetic Rain sub-parallel faults and antithetic left-lateral northeast-striking conjugate structures. The event is documented by fault geometries, flower structures, folds and predicted angular relationships following simple shear models for strike slip. The faults provided critical conduits for hydrothermal fluids. Interaction between the fault sets coupled with folding and low angle faulting also enhanced permeability in Webb Formation sediments.

Permeability at the Devils Gate Limestone-Webb Formation contact was also likely enhanced by paleokarst collapse breccias. Such features are present regionally in the Eastern Great Basin, resulting from exposure and erosion of the Devils Gate Limestone prior to Webb Formation deposition (Maher, 1997).

Stage 1 ends with introduction of hydrothermal fluids into the northeast- and northwest-striking fault sets and fluid migration into the permeable Devils Gate Limestone-Webb Formation contact horizon.

Stage Two: Hydrothermal Brecciation

Paragenetic relationships indicate that early fluids passively silicified Webb Formation sedimentary rocks. Passive silicification was followed by development of hydrothermal biotite. Biotite growth was followed by development of quartz, pyrite, arsenopyrite, arsenian-pyrite, sphalerite and realgar veins. These early events may have formed a low permeability cap in Webb Formation sediments. Dolomitization of the upper Devils Gate Limestone, especially near the Rain fault, may also be attributed to early hydrothermal fluids. Volume loss associated with dolomitization would have further enhanced permeability and generated open-space on the Devils Gate Limestone surface.

Early boiling and over-pressuring created dilatent fractures rather than fluidized breccia. This was due to relatively low available energy, the critical factor in determining if hydraulic fracturing leads to fluidized brecciation or if energy is dissipated by fluid loss through open fractures (Nelson and Giles, 1985). The hydraulic fracturing event resulted in the loss of water vapor from the system. Decreased water content of the remaining fluids resulted in supersaturation and rapid precipitation of stable mineral phases (Baker *et al.*, 1986) forming stage one veins. Early silicification and veining was followed by the first brecciation event.

Hydrothermal brecciation began with another high temperature fluid influx spreading onto the permeable Webb Formation-Devils Gate Limestone contact. Boiling was initiated, possibly triggered by decreasing depth and lithostatic pressure or seismic movements. Evidence of boiling includes highly variable fluid inclusion liquid to vapor ratios. Brecciation resulted when the boiling fluid became over-pressured. Such over-pressuring can result from the presence of a sealed cap, like that provided by early silicification and veining (Nelson and Giles, 1985). Initial boiling and over-pressuring resulted in hydrothermal fracturing which decreases the confining pressure on the water

column at depth, triggering increased boiling and initiating a chain reaction (Baker *et al.*, 1986). Movement of boiling-derived vapors through intensely fractured rocks ultimately resulted in fluidization.

Fluidization occurs when a liquid or gas is passed upward through a particulate bed, initially buoying the particles up in a condition similar to quicksand (Baker *et al.*, 1986). A fluidized state is attained when fluid velocity creates enough drag on particles to lift or suspend them against the force of gravity (McCallum, 1985). With increasing fluid velocity, particles become agitated and then transported upward through the center and down along the margins of the fluidized cell (Baker *et al.*, 1986). Textures attributable to fluidization at Rain include well rounded breccia fragments, abundant rock flour matrix locally exhibiting flow orientation (Fig. 13-C), and thorough mixing of fragment types derived from above and below the observed breccia (McCallum, 1985). The fluidization process also requires open space for fragments to be displaced relative to each other. At depths below 1 km such space can be provided by fracturing and doming of overlying units (Baker *et al.*, 1986; McCallum, 1985; Woolsey, 1973). At Rain paleokarst breccias and/or hydrothermal dolomitization and volume loss may have provided the open space. There is no evidence that the Rain hydrothermal breccia vented to the surface. Hydrothermal breccia bodies like Rain may not breach the surface due to the transition from dominantly vertical to dominantly horizontal stress regimes within the 0.5 to 1.0 km depth range (Baker *et al.*, 1986). Breccias formed at the vertical-horizontal stress transition range may flare out horizontally, similar to the Rain hydrothermal breccia. If the hydrothermal breccia does not breach the surface, however, a pressure differential through the breccia column is still required to sustain the fluidized cell. Such a pressure gradient may result from escape of volatiles to the surface via a network of fractures or even accretionary lapilli-bearing rock flour dikes (Baker *et al.*, 1986).

Textural and paragenetic relationships indicate the Rain breccia experienced multiple phases of boiling and over-pressuring during stage two. The fluidized breccia A event was followed by at least two more fluidized episodes, forming breccias B and C. Flow lineation orientations in breccias B and C vary widely indicating intense chaotic convective milling. Each boiling and brecciation event would have resulted in fluid supersaturation and rapid precipitation of breccia cement. The cement would seal the system, preparing it for another cycle of overpressuring and brecciation. Argillization of overlying Webb sediments due to condensing steam may have occurred throughout the brecciation process (Fig. 14).

Crackle breccia formed during all three brecciation events, due to hydrothermal overpressuring causing dilatent hydraulic fracturing and rock flour injection. The formation of fractured and weak rocks on the hydrothermal breccia margins facilitated further scouring during each brecciation event, progressively expanding the breccia body.

Minor gold precipitation may have occurred during one or all of the breccia events, resulting in low gold grade observed throughout the breccia (Fig. 14). The primary gold precipitation forming the high-grade underground orebody, however, is interpreted as occurring near the end of breccia C formation (Fig. 14), before or during cementation (after which the breccia was impermeable). The sharp grade boundary at the bottom of the high-grade zone suggests a late boiling horizon. The presence of highest grades in upper crackle and fluidized breccia suggests fluid ponding under the impermeable clay cap.

Stage Three: Late Stage Channelized Fluidization

Stage three began as turbulently fluidized brecciation ceased. As a hydrothermal system's energy decreases, fluid flow may become channelized along narrow conduits (McCallum, 1985). At Rain, gases generated by late boiling were channeled into conduits along northeast- and northwest-

striking faults and horizontal fractures created by pressure-decrease-related breccia subsidence. Channelized low-pressure flow resulted in formation of accretionary lapilli localized in pipe-, dike-, and sill-like bodies and emplacement of tuffisite dikes. The lapilli and tuffisite zones cut breccia C (Fig. 14).

Accretionary lapilli form when fluids vent through cohesive clay-sized material (McCallum, 1985). At Rain, fine material was provided by hydrothermal breccia rock flour matrix, further milled by channelized fluidization. Lapilli form by accretion of electrostatically charged fine sand and clay particles to a central grain and each other (McCallum, 1985; Woolsey, 1973; Baker *et al.*, 1986). Rain lapilli are dominated by tangentially-arranged highly-chargeable clay particles, while matrix material is relatively enriched in slightly coarser barite, pyrite and quartz grains. Lapilli are suspended by fluid streaming and grow by progressive enlargement during agitation and rotation (McCallum, 1985; Woolsey, 1973). Rain lapilli exhibit compositional and fragment size layering as a result of the enlargement process. Woolsey (1973) and McCallum (1985) noted that, in dry gas experiments, lapilli like those described at Rain could form without venting to the surface.

In experimental runs, Woolsey (1973) also noted that blocks from the walls of lapilli pipes were pulled into the conduit during continued fluidization. Slumping of material into conduits also resulted from compaction during phases of decreased gas pressure. The mechanism explains slumping and rotated blocks of lapilli breccias and sheared lapilli observed in the Rain pit exposures. Stage three was terminated by the end of boiling-induced fluidization as the system waned and cooled.

Stage Four: Post-Mineral Normal Faulting

The originally flat-lying Rain breccia and ore zones are bisected by normal offset on northeast-striking faults and, to a lesser extent, the Rain sub-parallel faults. The net effect is a series of rotated

blocks down-dropped to the northwest with local horsts and grabens developed by antithetic structures. The northeast-striking fault geometries match those described by Gans *et al.* (1985), Profett (1977) and Wernicke and Birchfiel (1982) for Basin and Range extensional fault sets. Stage four, then, is the effect of Basin and Range extensional tectonism.

Only minor normal reactivation (less than 7 m) occurred on the Rain fault set structures. The late motion formed the current subtle exposures of the faults cutting the breccia body. The northeast-striking fault set, in contrast, experienced significant reactivation with offsets up to 70 m. Some of the northeast-striking normal faults are reactivated versions of the original Rain fault strike-slip conjugate set. Most, however, resulted from stresses related to continuing rotational extension, regionally documented at 65 to 100% (Wernicke and Birchfiel, 1982).

Stage Five: Collapse Breccia Formation and Supergene Oxidation

Stage five occurred as acidic, oxidized fluids descended through the hydrothermal breccia along stage four normal faults, ponding on the Devils Gate Limestone surface. In the Rain pit orebody, sulfur isotope evidence indicates oxidation is supergene. The nature of oxidation at greater depths, however, is still under investigation.

Sulfur isotope ratios indicate that oxide products in the Rain pit resulted from supergene oxidation of hypogene and diagenetic sulfides. Supergene fluids oxidized diagenetic pyrite in Webb Formation rocks, forming acidic fluids. The fluids percolated down through the fluidized breccia along stage-four faults and fractures. The result was oxidation and argillization increasing downward toward the limestone contact. Coatings of kaolinite, halloysite, alunite, jarosite, duessertite and hematite were also deposited on faults and fractures throughout the orebody. The descending acidic fluids ponded on the Devils Gate Limestone contact and were buffered. As buffering occurred, elements that Rose *et al.* (1987) describe as soluble in acidic oxidized fluids but relatively insoluble

in neutral fluids (As, Hg, Co, Cu, Fe, Mn, Ni and Zn) were precipitated, forming the documented enrichments. Elements soluble in acidic oxidized fluids with precipitation triggered by reduction (V, Mo, and Sb) are also enriched on the limestone surface. The elements were acid-leached from the Webb Formation units and the breccia body, and precipitated due to buffering and reduction on the Devils Gate Limestone surface.

Fluid buffering also caused limestone dissolution and volume loss. The result was formation of collapse breccias observed on the Devils Gate Limestone contact under the breccia body. Breccia fragments are hydrothermal breccia, indicating post-mineral origin. Collapse breccias are unconsolidated and the matrix consists of insoluble residue and products of supergene argillic alteration, both resulting from acidic fluids. At the end of stage five, the Rain orebody was essentially as it is seen today.

Conclusions

On a world-wide scale, the Rain fluidized hydrothermal breccia body is unique, extending an amazing 5 km along strike. The hydrothermal system is zoned. The width of mineralization increases from the Rain pit northwest, widening dramatically in Zones 3 and 4 where a positive right-lateral flower structure has been documented. Grade also increases from the Rain pit northwest, and the percentage of barite decreases. The zoning suggests hydrothermal fluids were derived to the northwest. The zoning, combined with positive surface drill results from Northwest Rain and Tess indicate a promising future for Rain mine expansion.

The Rain system provides the best evidence to-date for right-lateral, strike-slip faulting as the critical element in formation of a Carlin Trend deposit. Evidence of multiple fluidized brecciation events is also unique to classic understanding about Carlin Trend deposits.

While our understanding has advanced, many aspects of the Rain system are still poorly understood. Refractory ore mineralogy, paragenesis and gold residence are being studied. The relationship between oxide and refractory mineralization, including the possibility of deep hypogene oxidation, is unclear. Future studies can also address Rain thermal and geochemical zoning and the role of organic carbon. These remaining puzzles will be the objective of Part II of this study, with completion expected in 1999.

Acknowledgements

Our current understanding of the Rain mineral system is built upon a strong foundation of sound geologic observations and interpretations by many Newmont geologists. D. McFarlane, G. Knutsen, R. Thoreson, J. Jory, M. Lane and D. Heitt made notable contributions toward understanding the Rain pit and underground orebody. Exploration geologists D. Mathewson, M. Jones, T. Longo and J. Read have and continue to expand our understanding of the system to the northwest. Drafting assistance from G. Heathman is greatly appreciated. Finally, Newmont management is acknowledged for their support of Rain research and this paper. The Ralph J. Roberts Center for Research in Economic Geology (CREG) at Mackay School of Mines, the University of Nevada, Reno, has provided support for part of this research.

References Cited

Arehart, G.B., Foland, K.A., Naeser, C.W., and Kesler, S.E., 1993, $^{40}Ar/^{39}Ar$, and fission track geochronology of sediment-hosted disseminated gold deposits at Post-Betze, Carlin Trend, northeastern Nevada: Economic Geology, v. 88, p. 622-646.

Baker, E.M., Kirwin, D.J., and Taylor, R.G., 1986, Hydrothermal breccia pipes: Economic Geology Research Unit, Contribution 12, James Cook University of North Canes, 35 p.

Christensen, O.D., 1993, Carlin Trend geologic overview: Gold deposits of the Carlin Trend, Nevada, *in* Society of Economic Geologist Field Trip Guidebook v. 18, p. 12-26.

Cole, D.M.,1995, Structural Evolution of the Gold Quarry Deposit and Implications for Development, Eureka County, Nevada: unpublished Colorado State University M.S. thesis, 79p.

Emsbo, P., Hofstra, A., Zimmerman, J.M.,and Snee, L., 1996, A mid-Tertiary age constraint on alteration and mineralization in igneous dikes on the Goldstrike property, Carlin Trend, Nevada, Geological Society of Nevada abstract with program.

Evans, J.G., 1980, Geology of the Rodeo Creek NE and Welches Canyon Quadrangles, Eureka County, Nevada: U.S. Geological Survey Professional Paper 1473, 81p.

Field, C.W., 1966, Sulfur isotopic method for discriminating between sulfates of hypogene and supergene origin: Economic Geology, v. 61, p. 14280-1433.

Gans, P.B., Miller, E.L, McCarthy, J., and Ouldcott, M.L., 1985, Tertiary extensional faulting and evolving ductile-brittle transition zones in the northern Snake Range and vicinity: New insights for seismic data: Geology, v. 13, p. 189-193.

Knutsen, G. and West, P., 1984, Geology of the Rain disseminated gold deposit, Elko county, Nevada: Arizona Geological Society Digest, v. 15, p. 73-76.

Maher, B., 1997, Mississippian sedimentary rock-hosted gold deposits of the eastern Great Basin: Relative importance of stratigraphic and structural ore controls: , *in* P. Vikre et. al. ed., Carlin-Type Gold Deposits Field Conference, Society of Economic Geologists Guidebook Series, v. 28, p.171-182.

McCallum, M.E., 1985, Experimental evidence for fluidization processes in breccia pipe formation: Economic Geology, v. 80, p. 1523-1543.

McClay, K.R., and Ellis, P.G., 1987, Geometries of extensional fault systems developed in model Experiments: Geology, v. 15, p. 341-344.

Nelson, C.E., and Giles, D.L., 1985, Hydrothermal eruption mechanisms and hot spring gold deposits: Economic Geology, v. 80, p. 1633-1639.

Nutt, C. J., 1997, Sequence of Deformational Events and the Recognition of Eocene (?) Deformation in the Alligator Ridge Area, East-central Nevada, *in* P. Vikre et. al. ed., Carlin-Type Gold Deposits Field Conference, Society of Economic Geologists Guidebook Series, v. 28, p. 203-221.

Odekirk, J.R., 1989, Age determination of alunite from jasperoid and an alteration pod within the Rain pit, Newmont Exploration Ltd., internal report, 5p.

Ohmoto, H., and Rye, R.O., 1979, Isotopes of sulfur and carbon, *in*: H.L. Barnes, ed., Geochemistry of Hydrothermal Ore Deposits, John Wiley and Sons, New York, p. 509-550.

Proffett, H.M., 1977, Cenozoic geology of the Yerington district, Nevada, and implications for the nature and origin of Basin and Range faulting: Geological Society of America Bulletin, v. 88, p. 247-266.

Putnam, B.R. III and Henriques, E.Q.B., 1991, Geology and mineralization at the South Bullion Deposit, Pinon Range, Elko County, Nevada: *in* G.L. Raines, R.E. Lisle, R.W. Schafer, an W.H. Wilkinson, Eds., Geology and Ore Deposits of the Great Basin: Geologic Society of Nevada Symposium Proceedings, Reno, p. 713-729.

Putnam, B.R. III and McFarlane, D., 1990, Western United States tectonics: evidence for wrench faulting from the Carlin Trend, Nevada: extended abstract for Penrose Conference on Transpressional Tectonics of Convergent Plate Margins, Bellingham, Washington, 4 p.

Rose, A.W., Hawkes H.E., and Webb J.S., 1987, Geochemistry in Mineral Exploration: Academic Press. pp. 549-583.

Rota, J.C., 1995, Gold Quarry: A Geologic Update, *in* Geological Society of Nevada, Field Trip Guidebook, Trip B - Structural Geology of the Carlin Trend, p. 67-78.

Shawe, D.R., 1965, Strike-slip control of Basin-Range structure indicated by historical faults in western Nevada: Geological Society of America Bulletin, v. 76, p. 361-1378.

Smith, J.F., and Ketner, K.B., 1968, Devonian and Mississippian Rocks and the Date of the Roberts Mountains Thrust in the Carlin-Piñon Range Area, Nevada: U.S. Geological Survey Bulletin 1251-I, 18p.

Smith, J.F., and Ketner, K.B., 1975, Stratigraphy of the Paleozoic Rocks in the Carlin-Piñon Range Area: U.S. Geological Survey Professional Paper 867, 87p.

Stewart, J.H., 1980, Geology of Nevada: Nevada Bureau of Mines and Geology, Special Publication 4, 136 p.

Sylvester, A.G., 1988, Strike-slip faults: Geological Society of America Bulletin, v. 100, p. 1666-1703.

Tchalenko, J.S., and Ambraseys, N.N., 1970, Structural analysis of the Dasht-e BaŶaz (Iran) earthquake fractures: Geological Society of America Bulletin, v. 81, p. 41-66.

Teal, L., and Jackson, M., 1997, Geologic overview of the Carlin Trend gold deposits and descriptions of recent deep discoveries: *in* P. Vikre et. al. ed., Carlin-Type Gold Deposits Field Conference, Society of Economic Geologists Guidebook Series, v. 28, p. 3-37.

Wernicke, B., and Burchfiel, B.C., 1982, Modes of extensional tectonics: Journal of Structural Geology, v. 4, no. 2., p. 105-115.

Wilcox, R.E., Harding, T.P., and Seely, D.R., 1973, Basic wrench tectonics: American Association of Petroleum Geologists Bulletin, v. 57, p. 74-96.

Williams, C.L., 1992, Breccia Bodies in the Carlin Trend, Elko and Eureka Counties, Nevada: Classification, Interpretation and Roles in Ore Formation, unpublished Colorado State University M.S. thesis, 213 p.

Woolsey, T.S., 1973, Physical modeling of diatreme emplacement: Unpublished Colorado State University M.S. thesis, 92 p.

10. Grade (grams) x thickness (meters) map extending from the Rain pit through zone 4 underground workings.

11. Average grade map extending from the Rain pit through zone 4 underground workings

12. Schematic geologic cross-section showing breccia types, dolomitized Devils Gate Limestone, and the gold orebody.

13. Photographs of Rain mine rock and core.

    A. Crackle breccia in carbonaceous Webb siltstone cemented by barite (white).

    B. Heterolithic matrix-supported hydrothermal breccia from Rain pit adjacent to the Sharpstone fault.

    C. Photomicrograph of flow-oriented fluidized matrix around breccia fragments and rounded quartz detritus, cut by irregular barite veinlets (white). Bar scale is 0.5mm.

    D. Photomicrograph of matrix barite euhedra and microcrystalline quartz matrix from hydrothermal Brecccia C stage. Bar scale is 0.5mm.

    E. Photomicrograph of pyrite (Py)-quartz vein fragment in Rain hydrothermal breccia. Bar scale is 0.1mm.

    F. Photomicrograqph of pyritized hydrothermal breccia fragment with diffusion banding indicating pyrite introduction after breccia development. Bar scale is 0.5mm.

    G. Accretionary lapilli (a) with slump flattening of lapilli (arrows) from tabular fluidized dikes in Rain open pit.

    H. Photomicrograph of silicified accretionary lapilli (a) with multiple concentric bands in fluidized and fragment-aligned hydrothermal breccia. Bar scale is 0.1mm.

14. Paragenetic sequence of gangue and ore minerals, breccia stages, and oxidation products from the oxidized portion of the Rain hydrothermal system.

15. Sulfur isotope ratios for diagenetic pyrite, hydrothermal pyrite, barite, and supergene alunite and jarosite from the Rain pit samples.

Figure 1. Williams, Thompson, Powell & Dunbar mns

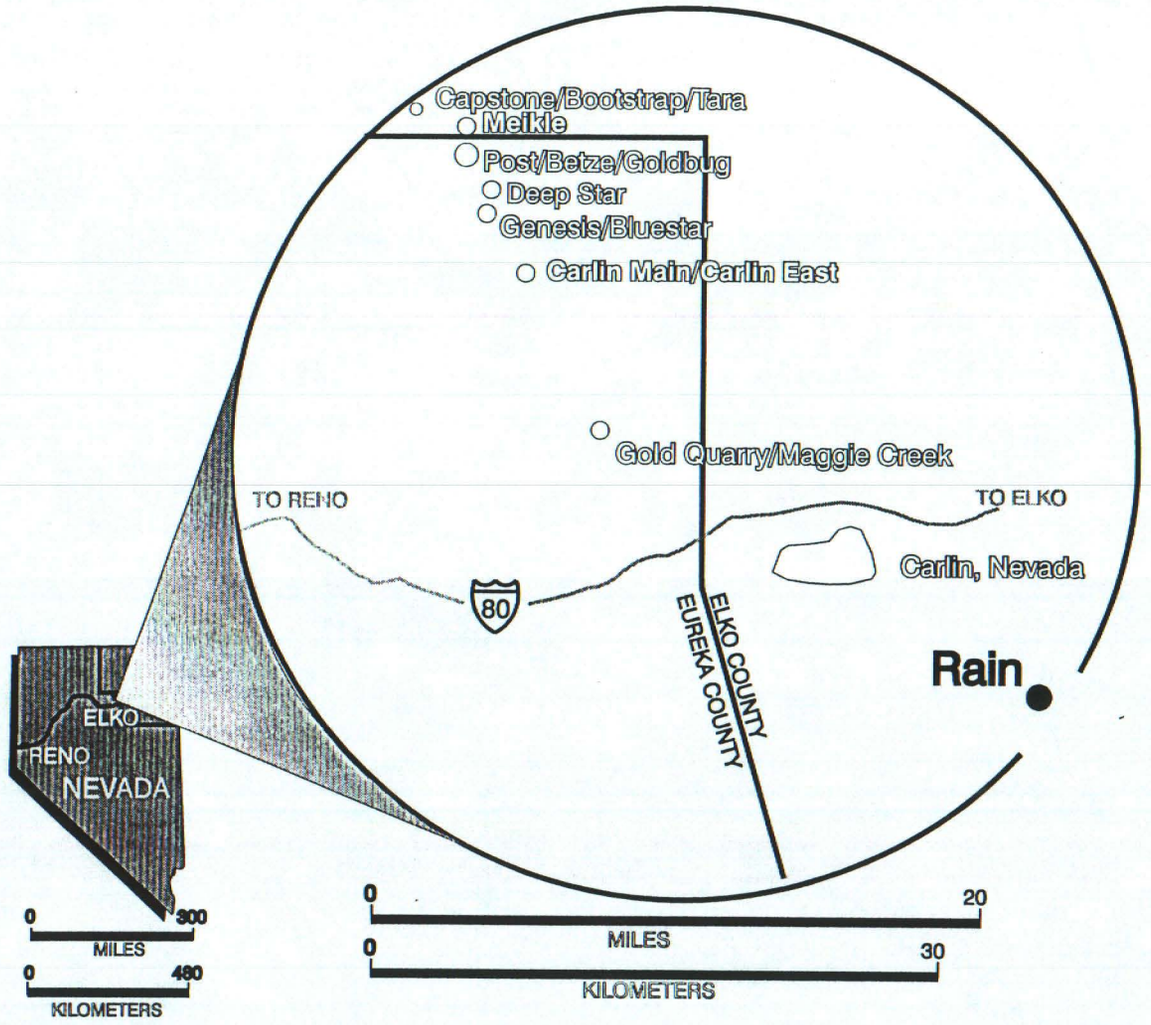

STRATIGRAPHIC COLUMN

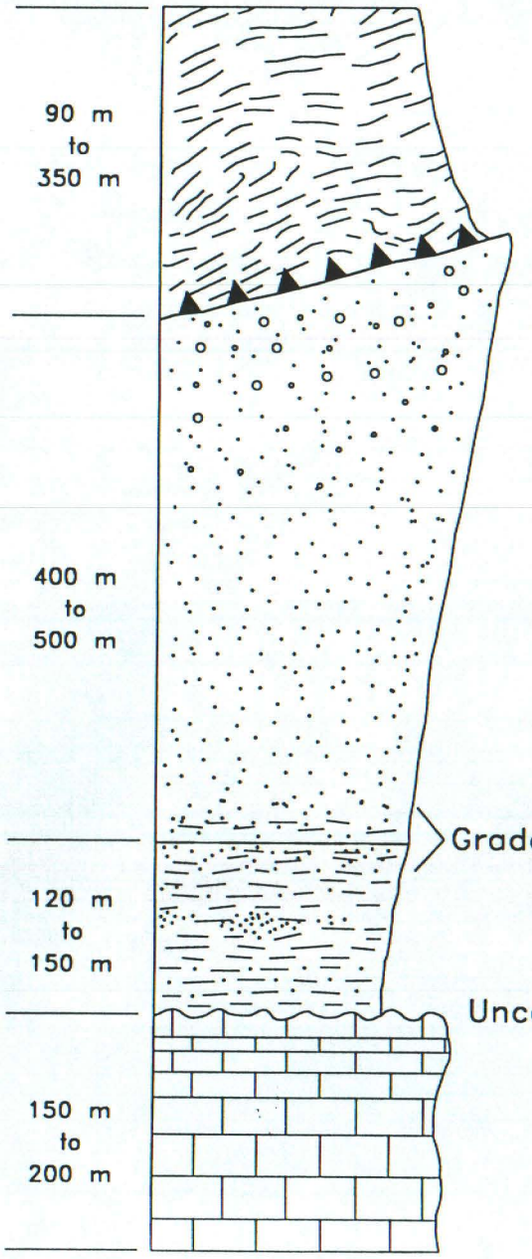

90 m to 350 m

Devonian Woodruff Formation
thin-bedded siltstone and mudstone

Roberts Mountains Thrust

400 m to 500 m

Mississippian Chainman Formation
medium- to coarse-grained sandstone and local conglomerate, coarsens upward

Gradational Contact

120 m to 150 m

Mississippian Webb Formation
thinly bedded mudstone and siltstone with local channel sandstone and conglomerate, coarsens upward

Unconformity

150 m to 200 m

Devonian Devils Gate Limestone
medium- to thick-bedded micritic limestone

Figure 3. Williams, Thompson, Powell & Dunbar mine

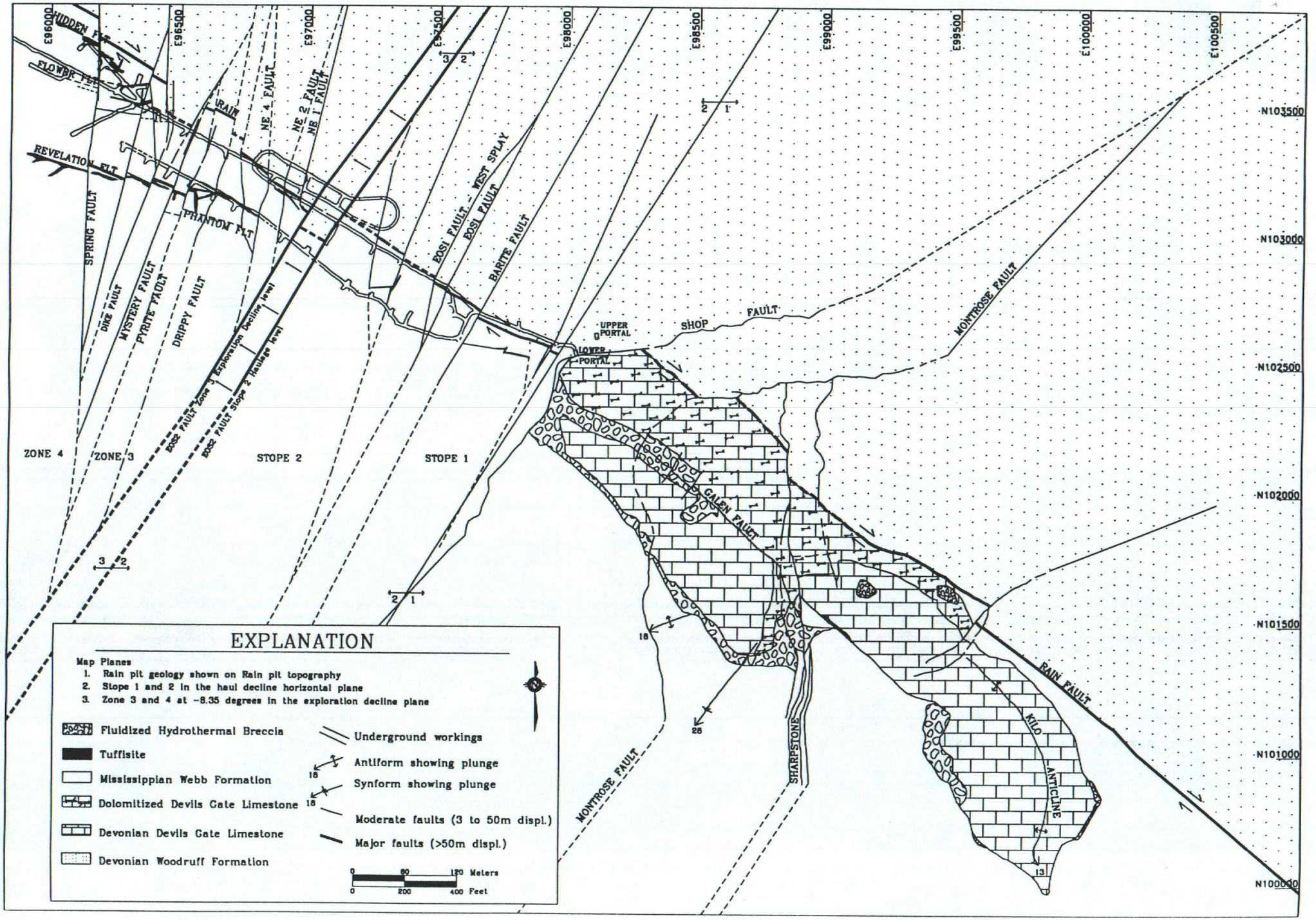

Figure 4. Williams, Thompson, Powell & Dunbar mns

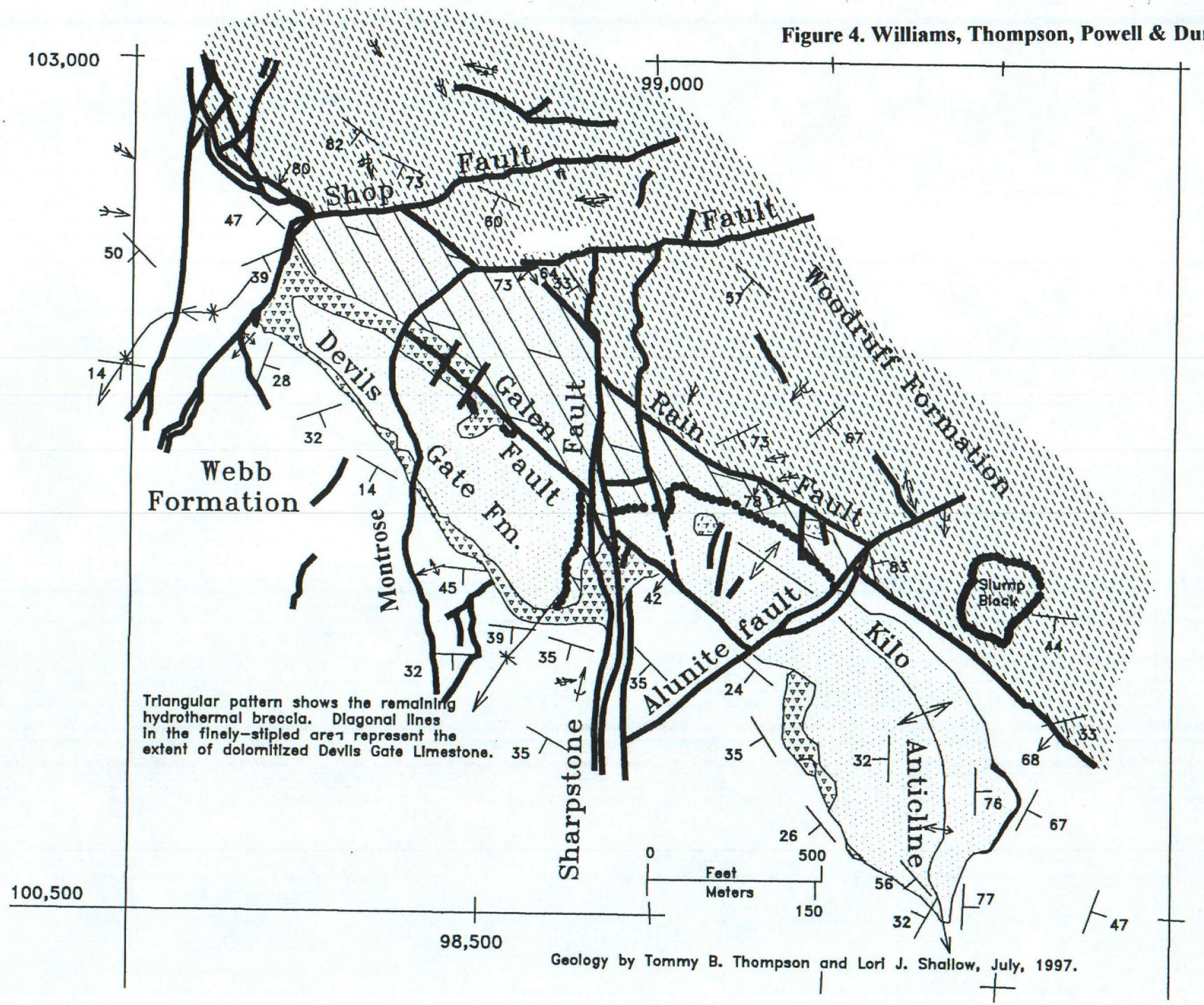

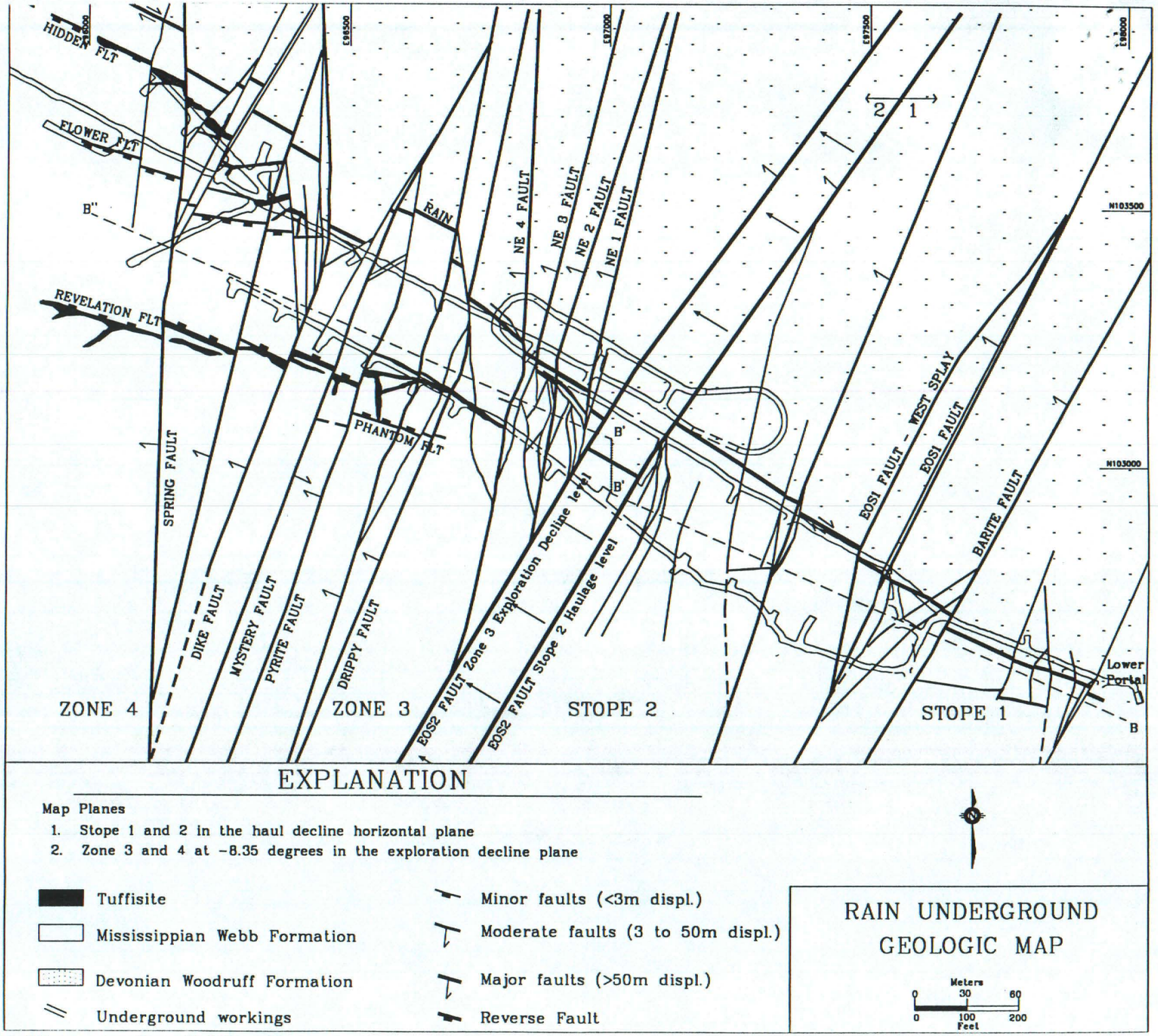

Figure 5. Williams, Thompson, Powell & Dunbar mns

Figure 10. Williams, Thompson, Powell & Dunbar mns

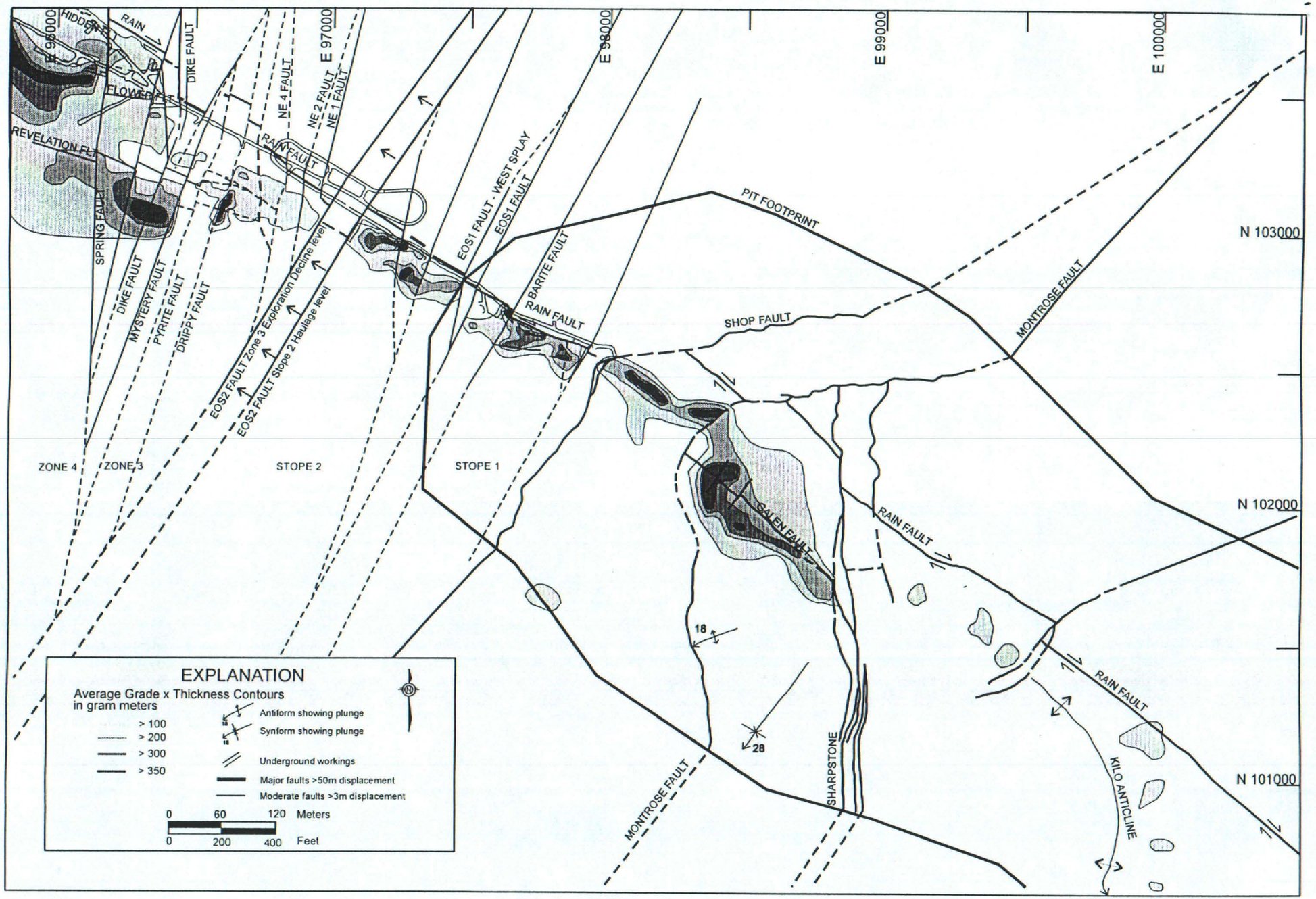

Figure 14. Williams, Thompson, Powell & Dunbar mns

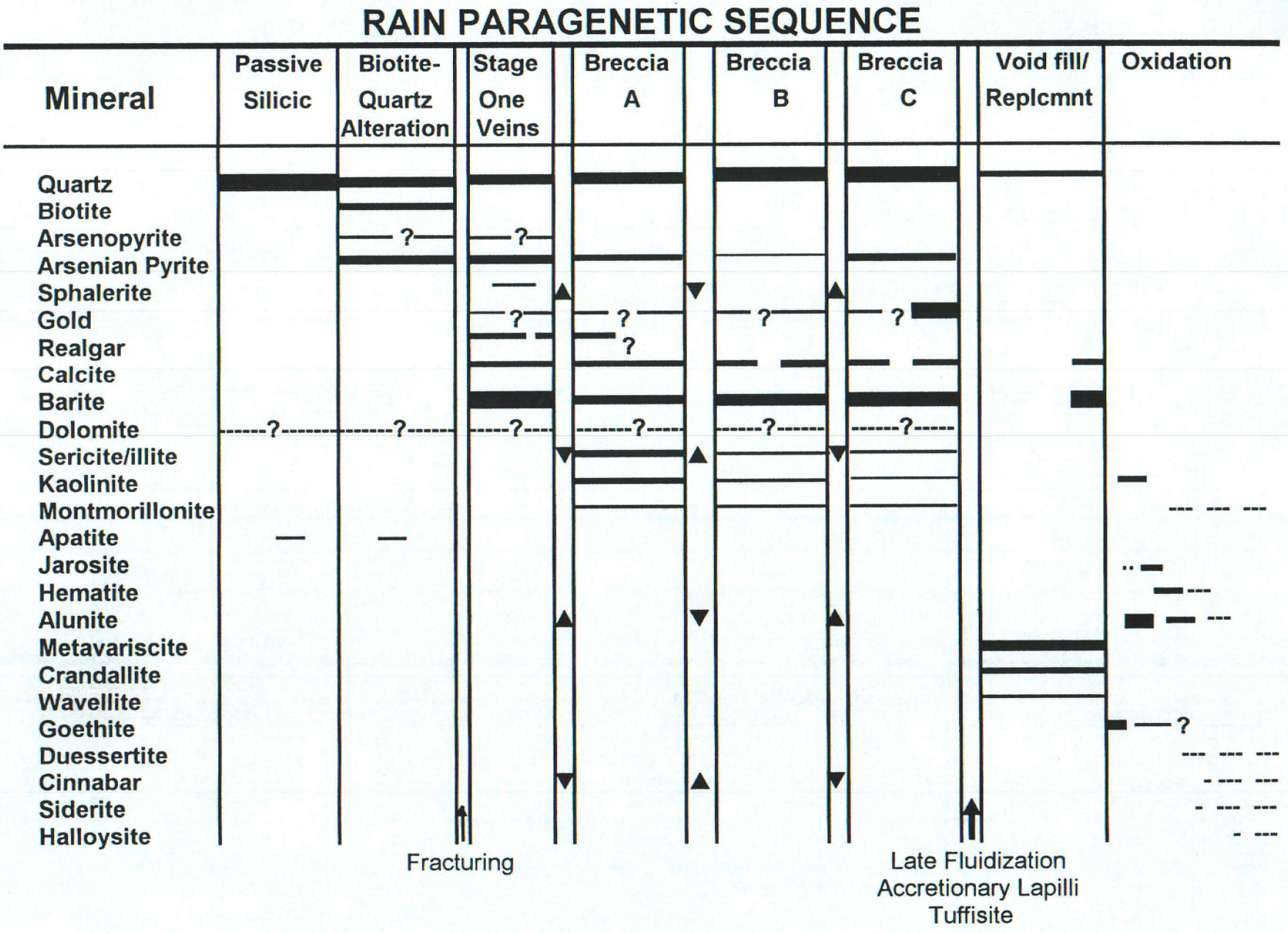

Figure 15. Williams, Thompson, Powell & Dunbar mns